

Gated Removal of Normalization in Transformers Enables Stable Training and Efficient Inference

Andrei Kanavalau¹ Carmen Amo Alonso² Sanjay Lall¹

Abstract

Normalization is widely viewed as essential for stabilizing Transformer training. We revisit this assumption for pre-norm Transformers and ask to what extent sample-dependent normalization is needed inside Transformer blocks. We introduce *TaperNorm*, a drop-in replacement for RMSNorm/LayerNorm that behaves exactly like the standard normalizer early in training and then smoothly tapers to a learned sample-independent linear/affine map. A single global gate is held at $g=1$ during gate warmup, used to calibrate the scaling branch via EMAs, and then cosine-decayed to $g=0$, at which point per-token statistics vanish and the resulting fixed scalings can be folded into adjacent linear projections. Our theoretical and empirical results isolate scale anchoring as the key role played by output normalization: as a (near) 0-homogeneous map it removes radial gradients at the output, whereas without such an anchor cross-entropy encourages unbounded logit growth (“logit chasing”). We further show that a simple fixed-target auxiliary loss on the pre-logit residual-stream scale provides an explicit alternative anchor and can aid removal of the final normalization layer. Empirically, TaperNorm matches normalized baselines under identical setups while eliminating per-token statistics and enabling these layers to be folded into adjacent linear projections at inference. On an efficiency microbenchmark, folding internal scalings yields up to $1.22\times$ higher throughput in last-token logits mode. These results take a step towards norm-free Transformers while identifying the special role output normalization plays.

1. Introduction

Normalization layers combined with residual connections were instrumental in making very deep networks trainable. Residual paths preserve gradients (He et al., 2015) while normalization layers such as BatchNorm, LayerNorm, and RMSNorm stabilize activations (Ioffe & Szegedy, 2015; Ba et al., 2016; Zhang & Sennrich, 2019). The latter two are commonly used in Transformer based language models where normalization is applied per-token. Per-token normalization introduces a data-dependent nonlinearity into every sublayer and incurs a computational cost because per-token statistics must be computed. It can also hinder mechanistic interpretability because it obscures the meaning of the residual-stream and makes it harder to decompose models into circuits (Baroni et al., 2025). This work examines whether per-token normalization in every Transformer block is necessary. The aim is to exploit normalization during the unstable early phase of training while ultimately producing a model that is norm-free and therefore simpler and cheaper at inference.

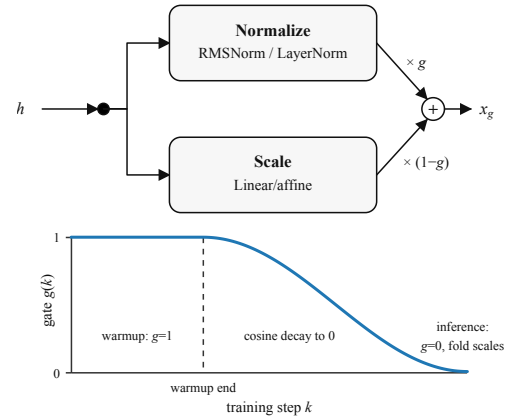


Figure 1. TaperNorm layer and gate scheduling.

To this end we introduce a gated layer, *TaperNorm*, that begins as ordinary RMSNorm/LayerNorm and then tapers to a simple sample-independent linear/affine map. A single global gate controls TaperNorm behavior such that early in training the model behaves exactly like a pre-norm Transformer. As the gate decays, normalizers are smoothly replaced by sample-independent scaling. At convergence,

¹Department of Electrical Engineering, Stanford University, Stanford, USA ²Department of Computer Science, Stanford University, Stanford, USA. Correspondence to: Andrei Kanavalau <kanaval@stanford.edu>.

per-token statistics are no longer used in the tapered layers. In our default setting we keep the final normalization active as an implicit scale anchor, but we also show that an explicit scale anchor, namely a fixed-target auxiliary loss on the pre-logit residual stream, can replace the final normalization. This enables all normalization layers to be tapered away.

Our mathematical analysis clarifies that what governs these behaviors is scale anchoring at the output. A final normalization layer is a convenient implicit anchor that removes radial gradients at the output, so the loss cannot be reduced by simply inflating the last hidden-state norm. Without such an anchor, cross-entropy has a radial component that drives logit magnitudes upward (“logit chasing”). We show that the fixed-target auxiliary loss introduces a counteracting radial restoring force, explaining why it can suppress logit chasing even when the final normalization is removed.

Removing per-token normalization is useful primarily at inference time. It has the potential to reduce computational costs of inference and aid interpretability efforts. In our approach, at the end of training each TaperNorm becomes a fixed linear or affine map, so its effect can be absorbed into adjacent linear projections (e.g. attention and MLP input projections).

Our key contributions are:

- A drop-in gated layer that transitions from tokenwise normalization to a fixed linear or affine rescaling, enabling removal of per-token statistics and operator fusion at inference.
- Analysis of pre-norm Transformers in which the final normalization acts as an implicit scale anchor that removes radial gradients, cross-entropy induces logit chasing without an anchor, and a fixed-target scale loss provides an explicit restoring force.
- Experiments on TinyStories and GPT-2 showing competitive loss while tapering normalization, and up to $1.22\times$ inference throughput improvements.

2. Related Work

Normalization has been central to stabilizing deep networks. BatchNorm improves optimization by normalizing intermediate activations (Ioffe & Szegedy, 2015), while LayerNorm removes batch coupling and became standard in sequence models (Ba et al., 2016). In Transformers, the pre-norm configuration, where input to each sublayer is normalized, improves stability over the original post-norm, where the residual stream is normalized after every sublayer contribution (Xiong et al., 2020). RMSNorm retains scale normalization but omits mean subtraction (Zhang & Sennrich, 2019) achieving a reduction in computational cost.

Two lines of work reduce reliance on per-token normalization. One replaces it via special initialization or residual scaling—Fixup (Zhang et al., 2019), ReZero (Bachlechner et al., 2020), LayerScale (Touvron et al., 2021), and DeepNorm (Wang et al., 2022). The other pursues normalizer-free training by modifying activations or attention: NF-Nets for ConvNets (Brock et al., 2021); Deep Kernel Shaping and related transformer modifications (Martens et al., 2021; He et al., 2023); and dynamic element-wise nonlinearities such as DyT (Zhu et al., 2025). Our approach takes a different route: we keep standard pre-norm dynamics when optimization is most unstable, then taper internal normalizers to a fixed linear/affine rescaling learned from data. By default we retain the final normalization as a convenient implicit scale anchor, and we additionally show that a fixed-target scale loss can serve as an explicit anchor that helps stabilize the removal process and also enables tapering away the final normalization as well when internal normalization is removed.

Closest in spirit is the work by Baroni et al. (2025) who show that LayerNorm layers in GPT-2 can be removed with a staged procedure and small accuracy loss. We complement this with a single global taper that avoids staged layer-by-layer removal schedules and directly targets convenient removal of normalization layers.

Compared to norm-replacement nonlinearities such as DyT (Zhu et al., 2025), our taper converges to a linear or affine map that can be absorbed into adjacent projections and removed from the inference graph. Compared to residual-scaling or initialization-based approaches (e.g. Fixup, ReZero, LayerScale, DeepNorm), our mechanism targets the normalization operator directly while keeping standard pre-norm behavior during the early phase. Finally, relative to staged LayerNorm removal in GPT-2 (Baroni et al., 2025), the single global taper avoids sequential layer schedules and is applicable to model pre-training.

3. Method

We study pre-norm Transformers and introduce a dynamic normalization layer *TaperNorm* that enables standard normalized dynamics during early training while enabling inference with fewer normalization operations. TaperNorm is a drop-in replacement for tokenwise RMSNorm or LayerNorm. It computes a convex combination of a standard normalization branch and a sample-independent scaling branch. A single scalar gate value $g(k) \in [0, 1]$ shared across layers and tokens at training step k interpolates between the branches. We keep $g(k) = 1$ during an initial gate warmup period so the model matches the normalized baseline while we accumulate exponential moving average (EMA) statistics. At the end of this period (the taper start), each TaperNorm layer sets a per-layer coefficient c from

these EMAs, copies per-feature scales from the normalization branch, and then freezes c . After taper start, $g(k)$ is cosine-decayed until $g = 0$. When $g = 0$ the layer becomes linear/affine, so it can be folded into adjacent linear projections for inference.

3.1. Pre-norm Transformer and notation

We consider models with embedding size d and sequence length T . Let $H^{(0,0)} \in \mathbb{R}^{T \times d}$ denote the input to the first block. Each layer j has multi-head self-attention (MHSA) and a feedforward network (MLP). Writing $\text{Attn}(H; \theta_{j,A})$ and $\text{MLP}(H; \theta_{j,M})$ for these components, the pre-norm residual updates are

$$\begin{aligned} H^{(j,1)} &= H^{(j,0)} + \text{Attn}\left(\text{Norm}_j^A(H^{(j,0)}); \theta_{j,A}\right), \\ H^{(j,2)} &= H^{(j,1)} + \text{MLP}\left(\text{Norm}_j^M(H^{(j,1)}); \theta_{j,M}\right), \\ H^{(j+1,0)} &= H^{(j,2)}, \end{aligned}$$

for $j = 0, \dots, L - 1$. In the TinyStories pre-training experiments we use SwiGLU activations and RoPE positional encoding.

After the L layers, we apply an output map $\text{Norm}_{\text{final}}$ tokenwise. In our main experiments $\text{Norm}_{\text{final}}$ is a standard RMSNorm or LayerNorm. In ablations that remove output normalization, we implement $\text{Norm}_{\text{final}}$ as a tapered layer whose gate is decayed to $g = 0$ over training. We represent token vectors as row vectors, so linear maps act on the right. A learned projection $W_{\text{out}} \in \mathbb{R}^{d \times V}$ yields logits

$$z = \text{Norm}_{\text{final}}(H^{(L,0)}) W_{\text{out}} \in \mathbb{R}^{T \times V}.$$

For a token at position t , let $z_t \in \mathbb{R}^V$ denote the t -th row of z and let y_t be its target id. The token-level cross-entropy is $\ell(z_t, y_t) = -\log \text{softmax}(z_t)_{y_t}$.

3.2. LayerNorm and RMSNorm

Given token row vector $h \in \mathbb{R}^{1 \times d}$, LayerNorm and RMSNorm are

$$\begin{aligned} \text{LayerNorm}(h) &= \frac{h - \mu_h}{\sigma_h} D_\gamma + \beta, \\ \mu_h &= \frac{1}{d} \sum_{i=1}^d h_i, \quad \sigma_h = \sqrt{\frac{1}{d} \sum_{i=1}^d (h_i - \mu_h)^2 + \varepsilon}, \end{aligned} \tag{1}$$

$$\begin{aligned} \text{RMSNorm}(h) &= \frac{h}{r(h)} D_\gamma, \\ r(h) &= \sqrt{\|h\|_2^2/d + \varepsilon}, \end{aligned} \tag{2}$$

with learnable per-feature scales $\gamma \in \mathbb{R}^d$ (and bias $\beta \in \mathbb{R}^d$ for LayerNorm). We write $D_\gamma := \text{diag}(\gamma)$ and $D_{\tilde{\gamma}} := \text{diag}(\tilde{\gamma})$ for diagonal scalings.

3.3. TaperNorm

TaperNorm dynamically transitions from RMSNorm/LayerNorm to a fixed linear or affine map of features. For gate $g \in [0, 1]$ and token $h \in \mathbb{R}^{1 \times d}$,

$$\text{TaperNorm}(h; g) = g \frac{h}{r(h)} D_\gamma + (1 - g) c h D_{\tilde{\gamma}}, \tag{3}$$

where $r(h)$ is as in RMSNorm, $c \in \mathbb{R}$ is a per-layer scalar, and $\tilde{\gamma} \in \mathbb{R}^d$ is a per-feature gain that remains trainable during tapering. The LayerNorm variant, used in GPT-2 experiments, is analogous and can be found in Appendix B. For $g = 1$ we recover RMSNorm/LayerNorm. For $g = 0$ we obtain a sample-independent scaling that can be fused into downstream linear operations.

We keep $g(k) = 1$ during an initial gate warmup period to obtain standard normalized dynamics and to accumulate EMA statistics used to set c . At the end of gate warmup (the taper start), each TaperNorm layer computes its own c^* from γ -weighted EMAs (Section 3.4), freezes this scalar for the remainder of training, and initializes $\tilde{\gamma} \leftarrow \gamma$. Both γ and $\tilde{\gamma}$ remain trainable and continue to update until convergence. After taper start, $g(k)$ is cosine-decayed from 1 to 0. This same scalar $g(k)$ is applied to every TaperNorm layer that is being tapered. At convergence, $g = 0$ and per-token statistics are no longer used.

When $g = 0$, TaperNorm can be removed from the inference graph by weight folding. For the RMSNorm case, $\text{TaperNorm}(h; 0) = c h D_{\tilde{\gamma}}$. If the next operation is a linear map $x \mapsto xW$ (with an optional bias), then we can replace W by $c D_{\tilde{\gamma}} W$ and remove the explicit TaperNorm. The same folding applies to attention and MLP input projections. For the LayerNorm variant, the $g = 0$ map is affine and can be folded into a following linear layer as described in Appendix B.

TaperNorm can be used to replace any subset of normalization layers. In this work we primarily taper internal normalizers, since this yields major inference savings (Section 5.2) while remaining stable across runs. Tapering the final norm provides little additional speedup. We report All-Taper ablations to demonstrate fully norm-free inference and because this regime may be of interest beyond inference efficiency e.g. mechanistic interpretability.

3.4. Calibrating the scaling branch

TaperNorm interpolates between a normalized branch and a sample-independent scaling branch. When the gate begins to decay after warmup, we would like the two branches to agree as closely as possible so the interpolation does not introduce an avoidable distribution shift. We therefore align the scaling branch to the normalization branch at the warmup boundary by setting $D_{\tilde{\gamma}} \leftarrow D_\gamma$ and choosing a

single scalar c that best matches normalized activations in least squares

$$\begin{aligned} c^* &\in \arg \min_c \mathbb{E} \left[\left\| \frac{h}{r(h)} D_\gamma - c h D_\gamma \right\|_2^2 \right] \\ &= \frac{\mathbb{E}[\|h D_\gamma\|_2^2 / r(h)]}{\mathbb{E}[\|h D_\gamma\|_2^2]}. \end{aligned} \quad (4)$$

This matches the two inputs in energy under the layer's current scaling, not in raw coordinates. The derivation is given in Appendix A.5.

3.5. Fixed-target scale anchoring loss

In addition to the tapering mechanism, we use an auxiliary loss that anchors the scale of the pre-logit residual stream. When a final normalization is present, this stabilizes the residual-stream scale during tapering by reducing activation variance. When the final normalization is tapered away, it also provides an explicit alternative to the final norm's implicit scale anchoring. Let token vectors before the final normalization, rows of $H^{(L,0)}$, be denoted using h_t . Define a per-token scale statistic

$$s(h) = \begin{cases} r(h) = \sqrt{\|h\|_2^2/d + \varepsilon} & \text{for RMSNorm,} \\ \sigma_h = \sqrt{\frac{1}{d} \sum_{i=1}^d (h_i - \mu_h)^2 + \varepsilon} & \text{for LayerNorm.} \end{cases}$$

The auxiliary loss penalizes deviations of token scales from a single scalar target

$$\mathcal{L}_{\text{aux}} = \lambda \mathbb{E}_{b,t} (s(h_{b,t}) - s_{\text{tgt}})^2, \quad (5)$$

where (b, t) index batch elements and sequence positions, and the expectation is taken over non-padding tokens. While $g = 1$ (gate warmup) we track an EMA of the batch mean $\hat{s}_k = \mathbb{E}_{b,t}[s(h_{b,t})]$, and at taper start we freeze s_{tgt} to the bias-corrected EMA value. After taper start, s_{tgt} remains constant for the remainder of training. We train with the combined objective $\mathcal{L} = \mathcal{L}_{\text{CE}} + \mathcal{L}_{\text{aux}}$, where \mathcal{L}_{CE} is token-level cross-entropy.

4. Scale anchoring

This section isolates the mechanism that explains the training behavior we observe when removing normalization. It is control of the scale of the pre-logit representation. When per-token normalization is removed, the scale of the last hidden state becomes a degree of freedom that can drift during training. A final normalization layer anchors it implicitly. Our fixed-target scale loss anchors it explicitly.

We analyze a single token vector $h \in \mathbb{R}^{1 \times d}$ that is input to the output projection. The logits are

$$z = \text{Norm}_{\text{final}}(h) W_{\text{out}} \in \mathbb{R}^{1 \times V}.$$

Only the radial component $\langle \nabla_h \ell(z, y), h \rangle$ can change $\|h\|_2$ to first order. The propositions below characterize this radial component for three cases that correspond to the design choices in our method. Proofs can be found in Appendix A.

Proposition 4.1 (Final normalization removes radial gradient). *Let the final map $\text{Norm}_{\text{final}}$ before the output projection be 0-homogeneous and differentiable almost everywhere. This includes the idealized RMSNorm and LayerNorm maps with $\varepsilon = 0$. For logits $z = \text{Norm}_{\text{final}}(h) W_{\text{out}}$ and any differentiable loss $\ell(z, y)$,*

$$\langle \nabla_h \ell(z, y), h \rangle = 0 \quad (h \neq 0).$$

Proposition 4.1 shows that normalization removes the radial gradient at the output. In this setting the loss cannot be reduced by simply rescaling the last hidden state.

Proposition 4.2 (Without the final norm, cross-entropy pushes norms up). *If $z = h W_{\text{out}}$ and ℓ is multiclass cross-entropy, then whenever the margin $m = z_y - \max_{j \neq y} z_j > 0$,*

$$\langle \nabla_h \ell(z, y), h \rangle = \langle \nabla_z \ell, z \rangle \leq -(1 - \text{softmax}(z)_y) m < 0,$$

so a small gradient step along $-\nabla_h \ell$ increases $\|h\|_2^2$ to first order.

Proposition 4.2 captures a simple mechanism for unbounded scale growth when the final normalization is removed. Once the correct class has positive margin, scaling logits along their current direction reduces cross-entropy. We refer to this tendency toward increasing confidence through logit magnitude as logit chasing.

Proposition 4.3 (Fixed-target scale loss provides a radial restoring force). *Let $r(h) = \sqrt{\|h\|_2^2/d + \varepsilon}$ and define the fixed-target auxiliary loss on a token vector h by*

$$\mathcal{L}_{\text{aux}}(h) = \lambda (r(h) - s_{\text{tgt}})^2, \quad \lambda > 0.$$

Then

$$\begin{aligned} \nabla_h \mathcal{L}_{\text{aux}}(h) &= \frac{2\lambda (r(h) - s_{\text{tgt}})}{d r(h)} h, \\ \langle \nabla_h \mathcal{L}_{\text{aux}}(h), h \rangle &= \frac{2\lambda (r(h) - s_{\text{tgt}})}{d r(h)} \|h\|_2^2. \end{aligned}$$

In particular, if $r(h) > s_{\text{tgt}}$ then a small gradient step on \mathcal{L}_{aux} decreases $\|h\|_2$ to first order; while if $r(h) < s_{\text{tgt}}$ it increases $\|h\|_2$.

Proposition 4.3 shows that the auxiliary loss injects an explicit restoring force on scale. For LayerNorm with $s(h) = \sigma_h$, the same conclusion holds with the restoring direction given by the mean-centered vector. The derivative formulas are given in Appendix A.4.

Taken together, Propositions 4.1–4.3 motivate our default training choices. Keeping the final normalization provides an implicit anchor that removes the radial component at the output. If we also taper away the final normalization, the fixed-target scale loss provides an explicit alternative that counteracts the radial push from cross-entropy.

5. Experiments

We evaluate TaperNorm in three settings. First, we pre-train pre-norm Transformers on TinyStories to test whether TaperNorm can match training with RMSNorm. Second, we run a microbenchmark to quantify inference gains from folding the resulting sample-independent scalings into adjacent projections. Third, we fine-tune GPT-2 models using the LayerNorm variant and compare to prior LayerNorm removal results.

5.1. Pre-training

We test pre-training performance on TinyStories with causal, pre-norm Transformers (depth 8, 16 attention heads at all widths, SwiGLU MLPs, RoPE) while varying width to obtain models at a range of scales from 1 to 30 million parameters. We repeat each configuration with 6 random seeds and report mean and standard deviation. Evaluation of models containing TaperNorm layers is performed with the gate set to 0, i.e. no per-token statistics used. Shaded regions in the plots indicate the 2.5–97.5 percentile range across seeds for each configuration.

All pre-training runs use a SentencePiece tokenizer trained on TinyStories (vocabulary size 10k) and a context length of 512 tokens. We use AdamW with peak learning rate 3×10^{-4} , $\beta = (0.9, 0.95)$, 5% linear warmup, and cosine decay to zero. We use no dropout or weight decay in these experiments.

Our default TaperNorm setting includes the fixed-target scale anchoring loss from Section 3.5. For ablations we also report runs without it. Among the taper variants, Internal-Taper (+aux) with the final RMSNorm retained is the most stable and reliable across seeds, and we use it as the default configuration in our main comparisons. We additionally report All-Taper (+aux) to quantify the fully norm-free setting enabled by explicit scale anchoring. For the 9M All-Taper (+aux) setting, one of the 6 seeds produced an unusually high validation loss, and we report statistics over the remaining 5 seeds (Table 2, [†]). The settings investigated are summarized in Table 1.

For all models containing TaperNorm layers we follow this gate schedule. During learning-rate warmup the gate is fixed at $g=1$. At the warmup boundary we compute c^* from γ -weighted EMAs with bias correction, copy $\gamma \rightarrow \tilde{\gamma}$, and then freeze c^* . Post-warmup, g is cosine-decayed to 0. All other

Table 1. Settings investigated for TinyStories pre-training. “Internal taper” and “Final taper” mean the corresponding normalization layers are replaced by TaperNorm.

Variant	Internal taper	Final taper	Scale loss \mathcal{L}_{aux}
Baseline (all RMSNorm)	✗	✗	✗
Internal-Taper	✓	✗	✗
Internal-Taper (+aux)	✓	✗	✓
Final-Taper	✗	✓	✗
All-Taper	✓	✓	✗
All-Taper (+aux)	✓	✓	✓

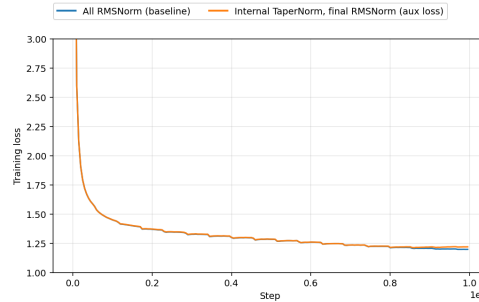


Figure 2. Training loss vs. step for the Baseline and Internal-Taper (+aux).

training details between same-size models are identical.

Figure 2 shows that with the final normalization kept in place, training loss trajectories for RMSNorm and TaperNorm are nearly indistinguishable. The only differences come near the end of training from the complete removal of per-token statistics in the internal layers. In Table 2 we report final validation losses for the Baseline, Internal-Taper (+aux), and All-Taper (+aux). Both taper variants track the baseline closely across scales: Internal-Taper (+aux) is within about 0.7–1.5% relative loss, while All-Taper (+aux) is within about 0.8–1.8%.

Figures 3 and 4 show that training dynamics are governed by scale anchoring at the pre-logit representation. Without an explicit anchor, removing the final normalization layer drastically alters optimization geometry with cross-entropy inducing rapid growth in logit magnitudes (logit chasing), consistent with Proposition 4.2. This effect is reflected in both activation-scale statistics and gradient magnitudes across parameter groups. When we enable the fixed-target scale loss from Section 3.5, the All-Taper model exhibits gradient magnitudes similar to those of the Internal-Taper model that keeps the final RMSNorm. This shows that explicit scale anchoring largely aligns the two.

5.2. Inference efficiency benchmarks

A key practical benefit of tapering normalization is that, once $g \rightarrow 0$, each TaperNorm becomes a sample-

Table 2. Validation loss for Baseline, Internal-Taper (+aux), and All-Taper (+aux). Percentages in parentheses show the relative gap vs. the Baseline. [†] For 9M All-Taper (+aux), we report mean \pm std over 5 seeds after excluding one outlier run with unusually high validation loss.

Model size	Baseline	Internal-Taper (+aux)	All-Taper (+aux)
1M	2.1538 ± 0.0025	2.1852 ± 0.0040 (+1.46%)	2.1930 ± 0.0035 (+1.82%)
3M	1.7561 ± 0.0010	1.7828 ± 0.0029 (+1.52%)	1.7874 ± 0.0028 (+1.78%)
9M	1.4620 ± 0.0022	1.4837 ± 0.0016 (+1.48%)	1.4837 ± 0.0023 [†] (+1.48%)
30M	1.2768 ± 0.0018	1.2859 ± 0.0010 (+0.71%)	1.2868 ± 0.0041 (+0.78%)

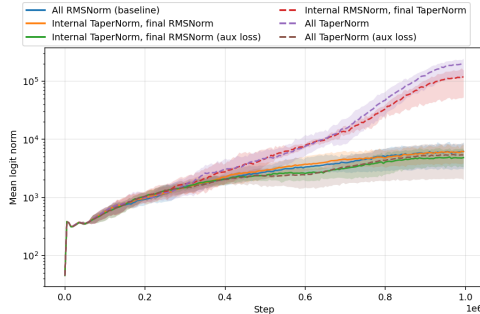


Figure 3. Mean logit ℓ_2 norm vs. step. Without a scale anchor, models with the final norm removed (dashed) can exhibit logit chasing, consistent with Proposition 4.2. With the fixed-target scale loss, logit growth is strongly suppressed in the All-Taper setting.

independent map and can be removed from the inference graph by folding its effect into adjacent linear projections. We quantify the resulting speedup on the TinyStories pre-trained Internal-Taper (aux) $d=512$ model ($\approx 30M$ parameters). We focus on the Internal-Taper model since this setting is more robust than All-Taper while providing near identical computational savings.

We benchmark on a single NVIDIA H100 80GB (CUDA 12.1, PyTorch 2.4.1+cu121) using bf16. We enable TF32 matmul where applicable. We time forward passes in last-token logits mode (only the final position’s logits are materialized), without KV caching, using token blocks sampled from the TinyStories validation split. Latency is averaged over 50 timed iterations after 10 warmup iterations using CUDA event timing, and throughput is reported in thousands of tokens per second (k tok/s).

We compare the following settings.

- **Baseline (RMSNorm).**
- **Internal-Taper (unfused)** where TaperNorm layers are exported to a fixed elementwise scaling but left as

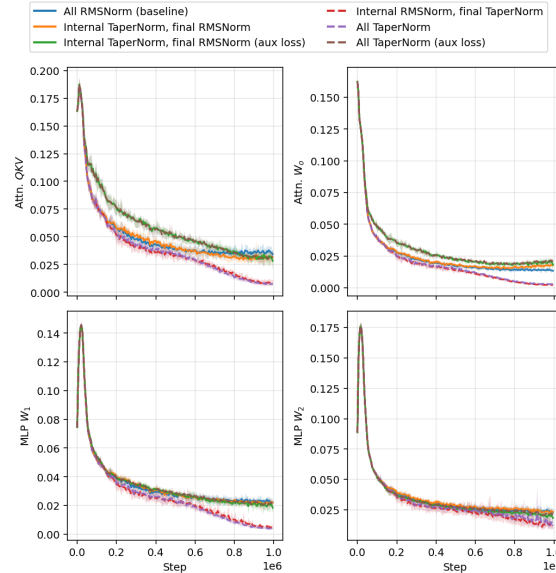


Figure 4. Average gradient norms across all Transformer blocks by weight type. Without explicit scale anchoring, gradients cluster primarily by presence vs. absence of the final normalization. With the fixed-target scale loss enabled, the gradient-magnitude gap between Internal-Taper and All-Taper largely disappears.

Table 3. Inference throughput (k tok/s, higher is better) in last-token logits mode on an NVIDIA H100 80GB (bf16, PyTorch 2.4.1+cu121, CUDA 12.1). Parentheses show speedup relative to the Baseline RMSNorm model.

Batch B	Seq. T	Baseline	Internal-Taper (unfused)	Internal-Taper (fused)
1	128	40.7	45.9 (1.13 \times)	48.7 (1.20 \times)
1	256	79.3	90.8 (1.14 \times)	96.8 (1.22 \times)
1	512	163.2	181.7 (1.11 \times)	195.5 (1.20 \times)
4	128	149.3	169.3 (1.13 \times)	180.4 (1.21 \times)
4	256	290.5	323.6 (1.11 \times)	344.9 (1.19 \times)
4	512	546.3	588.1 (1.08 \times)	615.9 (1.13 \times)

explicit operations.

- **Internal-Taper (fused)** where the internal scalings are folded into the attention QKV and MLP input projections, allowing normalization modules to be replaced by identity.

Table 3 reports inference throughput. Across the settings, the unfused TaperNorm model yields a consistent 1.08–1.15 \times throughput improvement over the RMSNorm baseline, while fully fusing the internal scaling into adjacent projections yields 1.13–1.22 \times throughput improvement. Gains are larger when per-token normalization is a larger fraction of the forward-pass cost, for example shorter sequences, while for larger T the attention and MLP compute become more significant.

5.3. Fine-tuning GPT-2 with TaperNorm

We fine-tune GPT-2 family models and compare to the LayerNorm removal results of Baroni et al. (2025). They show that LayerNorm layers in GPT-2 can be removed at inference time via fine-tuning with only a small increase in validation loss. Their key mechanism is to replace each LayerNorm with a linear surrogate, *FakeLN*, in which the per-token standard deviation σ is replaced by a single scalar σ_{avg} computed as the average of tokenwise standard deviations

$$\text{FakeLN}(x) = \frac{x - \mu}{\sigma_{\text{avg}}} D_\gamma + \beta.$$

Because removing all LayerNorm blocks simultaneously destabilizes the model, they adopt a sequential removal protocol. They remove one LayerNorm block at a time, fine-tuning for a fixed number of steps between removal events. They also introduce an auxiliary loss that encourages consistent tokenwise standard deviations across sequence positions

$$\mathcal{L}_{\text{Baroni}} = \lambda \mathbb{E}_{b,s} (\sigma_{b,s} - \hat{\sigma})^2, \quad \hat{\sigma} = \frac{1}{|\mathcal{M}|} \sum_{(b,s) \in \mathcal{M}} \sigma_{b,s},$$

where \mathcal{M} is a subset of token positions used to compute the average standard deviation $\hat{\sigma}$. Namely \mathcal{M} excludes the first token, padding tokens, and end-of-text positions. This auxiliary term is closely related to our scale-based view of normalization. The key difference from our fixed-target loss is that the target in $\mathcal{L}_{\text{Baroni}}$ is batch-dependent, so the loss does not pin an absolute pre-logit scale. Any constant value of $\sigma_{b,s}$ across positions yields zero penalty. Baroni et al. (2025) report that without this loss the fine-tuning loss curves during LN removal are more spiky. They also report that the auxiliary loss itself decreases quickly early in fine-tuning, which suggests that the model rapidly learns to equalize per-position scales. This behavior is consistent with scale control in Proposition 4.3 and with our empirical results. Our fixed-target loss instead anchors the pre-logit residual stream to a single absolute scale, which better aligns with our normalization replacement since the scaling branch learns its own gain.

We compare four settings.

- **Vanilla** (Baroni et al., 2025). Standard fine-tuned checkpoints with all LayerNorm layers intact.
- **FakeLN** (Baroni et al., 2025). We use the LayerNorm-free checkpoints published by the authors and evaluate them using their released code.
- **Internal-TaperLN (ours, +fixed-target aux)**. We replace every internal LayerNorm with TaperLN (Appendix B) and cosine-decay the shared gate to $g = 0$, while keeping the final LayerNorm active (locked at $g = 1$).

- **All-TaperLN (ours, +fixed-target aux)**. We replace all LayerNorm layers, including the final LayerNorm, with TaperLN and cosine-decay the shared gate to $g = 0$, yielding a fully norm-free model at inference.

We fine-tune on OpenWebText (Gokaslan et al., 2019), reuse the hyperparameters from Baroni et al. (2025) and set the tapering window by approximately aligning the end of warmup with their first LayerNorm removal step and the end of cosine gate decay with their first LayerNorm-free checkpoint. The exact schedule used is provided in Appendix D.

Table 4 reports end-of-run cross-entropy on OpenWebText, The Pile (Gao et al., 2020), and The Pile-filtered¹. Across GPT-2 Small, Medium, Large, and XL, Internal-TaperLN achieves losses comparable to the LayerNorm-free FakeLN checkpoints under the same overall fine-tuning recipe, while keeping the final LayerNorm as an implicit scale anchor. All-TaperLN yields a fully norm-free model and remains competitive with its losses comparable to (and sometimes better than) Internal-TaperLN, with a modest increase in some settings. In contrast to the staged FakeLN removal procedure, both taper protocols replace LayerNorm layers using a single global cosine gate and required no significant hyperparameter tuning in our experiments.

6. Discussion

The results and analysis identify scale anchoring as the key stabilizing role associated with output normalization in pre-norm Transformers. Scale anchoring controls the radial degree of freedom of the pre-logit representation. A final normalization layer provides a natural implicit anchor because normalization removes radial gradients at the output (Proposition 4.1). Without any anchor, cross-entropy induces logit chasing (Proposition 4.2). Our fixed-target scale loss provides an explicit alternative anchor by injecting a radial restoring force (Proposition 4.3).

This view explains the main training behaviors we observe when tapering normalization. When we remove the final normalization without an explicit anchor, logit norms grow and gradient magnitudes separate by the presence or absence of the final normalization. When we enable the fixed-target scale loss, this separation largely disappears. In particular, gradient magnitudes in All-Taper models become similar to those in Internal-Taper models that keep the final RM-SNorm. This supports the interpretation that the auxiliary term largely replaces the stabilizing effect of the final normalization when the model is otherwise being made norm-free.

¹The Pile-filtered consists of sequences from The Pile dataset, filtered by removing sequences containing tokens that appear in The Pile but not in OpenWebText (Baroni et al., 2025)

Table 4. End metrics on OpenWebText (OWT), The Pile, and The Pile-filtered for GPT-2 S/M/L/XL. Vanilla and FakeLN (+Baroni-aux) results follow Baroni et al. (2025). [†] Baroni et al. (2025) report that for GPT-2 XL LayerNorm free on The Pile, the mean CE loss can be dominated by a very small number of outlier sequences.

Model/Protocol	OWT	Pile	Pile-filtered
S/Vanilla	3.0126	2.8511	2.8112
S/FakeLN (+Baroni-aux)	3.0797	2.8852	2.8757
S/Internal-TaperLN (+fixed-target aux)	3.0584	2.8381	2.8374
S/All-TaperLN (+fixed-target aux)	3.0685	2.8326	2.8416
M/Vanilla	2.7390	2.5752	2.5724
M/FakeLN (+Baroni-aux)	2.7642	2.6579	2.6352
M/Internal-TaperLN (+fixed-target aux)	2.7550	2.5937	2.5936
M/All-TaperLN (+fixed-target aux)	2.7715	2.6248	2.6191
L/Vanilla	2.6240	2.6233	2.5074
L/FakeLN (+Baroni-aux)	2.6384	2.7504	2.5159
L/Internal-TaperLN (+fixed-target aux)	2.6277	2.7860	2.4910
L/All-TaperLN (+fixed-target aux)	2.6230	2.6539	2.4814
XL/Vanilla	2.4799	2.4673	2.3821
XL/FakeLN (+Baroni-aux)	2.5052	130.2197 [†]	2.3992
XL/Internal-TaperLN (+fixed-target aux)	2.5144	2.5303	2.3844
XL/All-TaperLN (+fixed-target aux)	2.5305	2.6504	2.4000

At deployment time, tapering is most useful because it turns normalization into a sample-independent map that can be absorbed into adjacent linear projections. This eliminates per-token statistics computation and enables operator fusion through weight folding. Section 5.2 shows that folding internal scalings yields 1.13–1.22× higher throughput in last-token logits mode on an NVIDIA H100.

7. Limitations and future work

Our experiments focus on pre-training up to 30M parameters on TinyStories and on fine-tuning GPT-2 family models. It remains to test how reliably the same tapering schedule and calibration procedure transfer to larger models, longer contexts, and a wider range of downstream tasks. Understanding which parts of the recipe are robust and which require tuning is an important direction for future work.

Our efficiency results are microbenchmarks on a single hardware and software stack (H100, PyTorch 2.4.1+cu121) and measure last-token forward passes without KV caching. End-to-end generation speedups may differ with caching, kernel availability, and compiler or runtime optimizations.

More broadly, our analysis emphasizes scale control at the pre-logit representation, but scale is not the only training

stability factor in deep Transformers. It remains to study how tapering interacts with other stabilizers and regularizers, including weight decay, dropout, and alternative anchoring penalties.

8. Conclusion

We introduced TaperNorm, a gated replacement for RMSNorm and LayerNorm that matches standard normalized behavior early in training and then transitions to a learned sample-independent rescaling. This transition removes per-token statistics at convergence and allows the resulting linear/affine operations to be folded into adjacent linear projections for inference.

Our analysis isolates scale anchoring at the output as the mechanism that explains the main training phenomena when output normalization is removed. A final normalization layer provides an implicit anchor by removing the radial component of the gradient, while without an anchor cross-entropy induces logit chasing. We further showed that a fixed-target scale loss provides an explicit alternative anchor by introducing a radial restoring force, which explains why it can suppress logit chasing when the final normalization is also tapered away.

Empirically, TaperNorm yields validation performance within about 2% of normalized baselines across model scales and produces competitive results when fine-tuning GPT-2 family models. In a bf16 NVIDIA H100 microbenchmark, folding internal scalings into adjacent projections yields up to 1.22× higher throughput in last-token logits mode.

References

Ba, J. L., Kiros, J. R., and Hinton, G. E. Layer normalization, 2016. URL <https://arxiv.org/abs/1607.06450>.

Bachlechner, T., Majumder, B. P., Mao, H. H., Cottrell, G. W., and McAuley, J. Rezero is all you need: Fast convergence at large depth, 2020. URL <https://arxiv.org/abs/2003.04887>.

Baroni, L., Khara, G., Schaeffer, J., Subkhankulov, M., and Heimersheim, S. Transformers don’t need layernorm at inference time: Scaling layernorm removal to gpt-2 xl and the implications for mechanistic interpretability, 2025. URL <https://arxiv.org/abs/2507.02559>.

Brock, A., De, S., Smith, S. L., and Simonyan, K. High-performance large-scale image recognition without normalization, 2021. URL <https://arxiv.org/abs/2102.06171>.

Gao, L., Biderman, S., Black, S., Golding, L., Hoppe, T.,

Foster, C., Phang, J., He, H., Thite, A., Nabeshima, N., Presser, S., and Leahy, C. The Pile: An 800GB dataset of diverse text for language modeling. *arXiv preprint arXiv:2101.00027*, 2020. doi: 10.48550/arXiv.2101.00027.

Gokaslan, A., Cohen, V., Pavlick, E., and Tellex, S. Openwebtext corpus. <http://Skylion007.github.io/OpenWebTextCorpus>, 2019.

He, B., Martens, J., Zhang, G., Botev, A., Brock, A., Smith, S. L., and Teh, Y. W. Deep transformers without shortcuts: Modifying self-attention for faithful signal propagation, 2023. URL <https://arxiv.org/abs/2302.10322>.

He, K., Zhang, X., Ren, S., and Sun, J. Deep residual learning for image recognition, 2015. URL <https://arxiv.org/abs/1512.03385>.

Ioffe, S. and Szegedy, C. Batch normalization: Accelerating deep network training by reducing internal covariate shift, 2015. URL <https://arxiv.org/abs/1502.03167>.

Martens, J., Ballard, A., Desjardins, G., Swirszcz, G., Dalibard, V., Sohl-Dickstein, J., and Schoenholz, S. S. Rapid training of deep neural networks without skip connections or normalization layers using deep kernel shaping, 2021. URL <https://arxiv.org/abs/2110.01765>.

Touvron, H., Cord, M., Sablayrolles, A., Synnaeve, G., and Jégou, H. Going deeper with image transformers, 2021. URL <https://arxiv.org/abs/2103.17239>.

Wang, H., Ma, S., Dong, L., Huang, S., Zhang, D., and Wei, F. Deepnet: Scaling transformers to 1,000 layers, 2022. URL <https://arxiv.org/abs/2203.00555>.

Xiong, R., Yang, Y., He, D., Zheng, K., Zheng, S., Xing, C., Zhang, H., Lan, Y., Wang, L., and Liu, T.-Y. On layer normalization in the transformer architecture, 2020. URL <https://arxiv.org/abs/2002.04745>.

Zhang, B. and Sennrich, R. Root mean square layer normalization, 2019. URL <https://arxiv.org/abs/1910.07467>.

Zhang, H., Dauphin, Y. N., and Ma, T. Fixup initialization: Residual learning without normalization, 2019. URL <https://arxiv.org/abs/1901.09321>.

Zhu, J., Chen, X., He, K., LeCun, Y., and Liu, Z. Transformers without normalization, 2025. URL <https://arxiv.org/abs/2503.10622>.

A. Proofs for Section 4

Preliminaries and assumptions

We recall $r(h) := \sqrt{\|h\|_2^2/d + \varepsilon}$ and $D_\gamma := \text{diag}(\gamma)$, $D_{\tilde{\gamma}} := \text{diag}(\tilde{\gamma})$. Expectations $\mathbb{E}[\cdot]$ are over mini-batch elements and sequence positions unless stated.

A.1. Proof of Proposition 4.1

Proof. A map Norm is 0-homogeneous if $\text{Norm}(\alpha h) = \text{Norm}(h)$ for all $\alpha > 0$ and $h \neq 0$. Differentiating in α at $\alpha = 1$ gives $\frac{d}{d\alpha} \text{Norm}(\alpha h) \big|_{\alpha=1} = h J_{\text{Norm}}(h) = 0$, so h lies in the left nullspace of the Jacobian $J_{\text{Norm}}(h)$. With $z = \text{Norm}_{\text{final}}(h) W_{\text{out}}$ we have by the chain rule

$$\nabla_h \ell(z, y) = \nabla_z \ell(z, y) W_{\text{out}}^\top J_{\text{Norm}}(h)^\top.$$

Taking the inner product with h ,

$$\langle \nabla_h \ell, h \rangle = \nabla_z \ell W_{\text{out}}^\top J_{\text{Norm}}(h)^\top h^\top = \nabla_z \ell W_{\text{out}}^\top (h J_{\text{Norm}}(h))^\top = 0.$$

The identity is exact for exactly 0-homogeneous maps. RMSNorm and LayerNorm satisfy this property in the limit $\varepsilon = 0$. \square

A.2. Proof of Proposition 4.2

Proof. For multiclass cross-entropy with softmax probabilities $p = \text{softmax}(z)$, $\nabla_z \ell = p - e_y$. Then

$$\langle \nabla_z \ell, z \rangle = \sum_i z_i (p_i - 1_{i=y}) = \sum_i p_i z_i - z_y = \mathbb{E}_p[z] - z_y.$$

Let $m = z_y - \max_{j \neq y} z_j > 0$ and $b = \max_{j \neq y} z_j \leq z_y - m$. Since $\sum_{j \neq y} p_j = 1 - p_y$ and $z_j \leq b$ for $j \neq y$,

$$\mathbb{E}_p[z] = p_y z_y + \sum_{j \neq y} p_j z_j \leq p_y z_y + (1 - p_y)b \leq p_y z_y + (1 - p_y)(z_y - m) = z_y - (1 - p_y)m.$$

Hence $\langle \nabla_z \ell, z \rangle \leq -(1 - p_y)m < 0$. With $z = h W_{\text{out}}$ and $\nabla_h \ell = \nabla_z \ell W_{\text{out}}^\top$, we have $\langle \nabla_h \ell, h \rangle = \langle \nabla_z \ell, z \rangle$. A gradient descent step $h^+ = h - \eta \nabla_h \ell$ therefore satisfies

$$\|h^+\|_2^2 - \|h\|_2^2 = -2\eta \langle \nabla_h \ell, h \rangle + O(\eta^2) \geq 2\eta(1 - p_y)m + O(\eta^2),$$

so the norm increases to first order. \square

A.3. Proof of Proposition 4.3

Proof. Let $r(h) = \sqrt{\|h\|_2^2/d + \varepsilon}$. Since $\nabla_h \|h\|_2^2 = 2h$, we have

$$\nabla_h r(h) = \frac{1}{2} (\|h\|_2^2/d + \varepsilon)^{-1/2} \cdot \frac{2h}{d} = \frac{h}{d r(h)}.$$

Therefore

$$\nabla_h \mathcal{L}_{\text{aux}}(h) = 2\lambda (r(h) - s_{\text{tgt}}) \nabla_h r(h) = \frac{2\lambda (r(h) - s_{\text{tgt}})}{d r(h)} h.$$

Taking the inner product with h yields the second identity, and the final statement follows from the first-order norm expansion $\|h - \eta \nabla_h \mathcal{L}_{\text{aux}}\|_2^2 = \|h\|_2^2 - 2\eta \langle \nabla_h \mathcal{L}_{\text{aux}}, h \rangle + O(\eta^2)$. \square

A.4. LayerNorm scale gradient formulas

Let $h \in \mathbb{R}^{1 \times d}$ be a token vector, let $\mu_h = \frac{1}{d} \sum_{i=1}^d h_i$, and define the mean-centered vector $\bar{h} := h - \mu_h \mathbf{1}$. Let

$$\sigma_h = \sqrt{\frac{1}{d} \|\bar{h}\|_2^2 + \varepsilon}.$$

Then

$$\nabla_h \sigma_h = \frac{\bar{h}}{d\sigma_h}.$$

Therefore, for the fixed-target auxiliary loss $\lambda(\sigma_h - s_{\text{tgt}})^2$,

$$\nabla_h (\lambda(\sigma_h - s_{\text{tgt}})^2) = \frac{2\lambda(\sigma_h - s_{\text{tgt}})}{d\sigma_h} \bar{h}.$$

This shows that the auxiliary term pulls σ_h toward s_{tgt} through a restoring force in the mean-zero subspace.

A.5. Derivation of c^* in (4)

Let $A(h) = \frac{h}{r(h)} D_\gamma$ and $B(h) = h D_\gamma$. The objective is

$$J(c) = \mathbb{E}[\|A(h) - cB(h)\|_2^2] = \mathbb{E}[\|A\|_2^2] - 2c\mathbb{E}[\langle A, B \rangle] + c^2\mathbb{E}[\|B\|_2^2].$$

Differentiating and setting to zero gives

$$0 = J'(c) = -2\mathbb{E}[\langle A, B \rangle] + 2c\mathbb{E}[\|B\|_2^2] \Rightarrow c^* = \frac{\mathbb{E}[\langle A, B \rangle]}{\mathbb{E}[\|B\|_2^2]} = \frac{\mathbb{E}[\|hD_\gamma\|_2^2/r(h)]}{\mathbb{E}[\|hD_\gamma\|_2^2]}.$$

A.6. EMA estimators for c^*

During warmup we estimate

$$\bar{a} = \mathbb{E}[\|hD_\gamma\|_2^2/r(h)], \quad \bar{b} = \mathbb{E}[\|hD_\gamma\|_2^2]$$

with exponential moving averages (EMAs) $s_{\text{num}}, s_{\text{den}}$ using an EMA update rate $\mu \in (0, 1)$ (i.e., μ is the new-sample weight). Concretely, for a stream of observations x_k we use

$$s \leftarrow (1 - \mu) s + \mu x_k, \quad s^{(0)} = 0.$$

After n updates, bias correction yields

$$\hat{s}_{\text{num}} = \frac{s_{\text{num}}}{1 - (1 - \mu)^n}, \quad \hat{s}_{\text{den}} = \frac{s_{\text{den}}}{1 - (1 - \mu)^n}, \quad c^* = \frac{\hat{s}_{\text{num}}}{\hat{s}_{\text{den}} + \delta},$$

with small $\delta > 0$ for numerical stability. After this assignment, c^* is frozen for the remainder of training.

B. LayerNorm version of TaperNorm (TaperLN)

This section provides the LayerNorm analogue of the RMSNorm formulation used in the main text, including the definition of the layer, the optimal alignment scalar c^* , EMA estimators, and the substitutions required for the theoretical results.

Definition. For a token row vector $h \in \mathbb{R}^{1 \times d}$, let

$$\mu_h = \frac{1}{d} \sum_{i=1}^d h_i, \quad \sigma_h = \sqrt{\frac{1}{d} \sum_{i=1}^d (h_i - \mu_h)^2 + \varepsilon}, \quad D_\gamma = \text{diag}(\gamma), \quad D_{\tilde{\gamma}} = \text{diag}(\tilde{\gamma}).$$

Our GPT-2 fine-tuning code uses a TaperLN module that interpolates between the standard LayerNorm branch and a mean-centered scaling branch:

$$\text{TaperLN}(h; g) = \beta + g \frac{h - \mu_h}{\sigma_h} D_\gamma + (1 - g) c(h - \mu_h) D_{\tilde{\gamma}}, \quad g \in [0, 1]. \quad (6)$$

For $g = 1$ the layer equals $\text{LayerNorm}(h)$; for $g = 0$ it becomes a fixed affine map built from mean subtraction and a featurewise scaling.

At $g = 0$, the map is affine in h : it equals $hA + \beta$ where $A = c(I - \frac{1}{d}\mathbf{1}\mathbf{1}^\top)D_{\tilde{\gamma}}$. Thus, for a following projection $x \mapsto xW + b$ we can fold the affine map into (W, b) .

Table 5. Total TinyStories pre-training steps by model width.

Width d	Total steps
64	500,000
128	500,000
256	750,000
512	1,000,000

Calibration of c (LayerNorm case). At the warmup boundary we align the $g = 0$ branch to the $g = 1$ LayerNorm branch by choosing c to minimize a one-dimensional least-squares objective analogous to (4), but with mean-centering and σ_h : let $\bar{h} := h - \mu_h \mathbf{1}$ and define

$$c^* \in \arg \min_{c \in \mathbb{R}} \mathbb{E} \left[\left\| \frac{\bar{h}}{\sigma_h} D_\gamma - c \bar{h} D_\gamma \right\|_2^2 \right] = \frac{\mathbb{E}[\|\bar{h} D_\gamma\|_2^2 / \sigma_h]}{\mathbb{E}[\|\bar{h} D_\gamma\|_2^2]}. \quad (7)$$

This is the exact analogue of (4) under the substitutions $h \mapsto \bar{h}$ and $r(h) \mapsto \sigma_h$.

EMA estimators and freezing. During warmup we track the numerator and denominator in (7) with EMAs and apply the same bias correction as in Appendix A.6. At the warmup boundary we set $c \leftarrow c^*$, copy $\gamma \rightarrow \tilde{\gamma}$, and freeze c for the remainder of training (while γ and $\tilde{\gamma}$ remain trainable; see Section 3.3).

Relationship to the RMSNorm variant. All statements in Section 4 hold for TaperLN under the same regularity assumptions after the substitutions

$$\frac{h}{r(h)} \longrightarrow \frac{h - \mu_h}{\sigma_h}, \quad \Delta(h) = c h D_{\tilde{\gamma}} - \frac{h}{r(h)} D_\gamma \longrightarrow \Delta_{\text{LN}}(h) = c(h - \mu_h) D_{\tilde{\gamma}} - \frac{h - \mu_h}{\sigma_h} D_\gamma.$$

In particular, Proposition 4.1 continues to apply because the ideal LayerNorm map (with $\varepsilon = 0$) is 0-homogeneous for positive scalings. If a bias β is included, it does not affect 0-homogeneity for $\alpha > 0$ because it is invariant to radial scalings; Proposition 4.1 therefore does not require $\beta=0$.

C. Training details

This appendix summarizes the TinyStories pre-training setup used in Section 5.

Data and tokenizer. We pre-train on TinyStories using a SentencePiece tokenizer trained on TinyStories with vocabulary size 10k. Training sequences are formed by sampling random contiguous windows of length $T = 512$ from a concatenated token stream. We train with next-token prediction using a one-token shift.

Model. All pre-training models are causal, pre-norm Transformers with depth $L = 8$. All widths use 16 attention heads, RoPE positional encoding, and SwiGLU MLPs with expansion factor 4. Linear layers in attention and MLP use no bias. Output weights are tied to the token embedding matrix. Dropout is disabled.

Optimization. We use AdamW with $\beta = (0.9, 0.95)$ and peak learning rate 3×10^{-4} . The schedule uses linear warmup for 5% of total steps followed by cosine decay to zero. We use no weight decay. We apply global gradient norm clipping with threshold 1.0. The batch size is 16 sequences of length 512.

Run lengths. Total training steps vary by model width as shown in Table 5. Warmup uses 5% of total steps for every run.

TaperNorm, EMA rates, and scale loss. For any layer that is tapered, we keep the gate at $g = 1$ during learning-rate warmup. At the warmup boundary, each tapered layer computes its alignment scalar c using γ -weighted EMA estimates of the quantities in Section 3.4, copies $\gamma \rightarrow \tilde{\gamma}$, and then freezes c . After warmup, we cosine-decay the shared gate value $g(k)$ from 1 to 0 over the remaining training steps.

Table 6. GPT-2 fine-tuning and taper schedule.

Model	total steps	warmup end k_w	taper start k_{start}	taper end k_{end}
GPT-2 Small	300	25	25	100
GPT-2 Medium	500	10	20	200
GPT-2 Large	600	30	30	500
GPT-2 XL	800	20	50	700

We use the same EMA update rate $\mu = 0.01$ (new-sample weight) for both (i) the calibration EMAs used to set c and (ii) the warmup EMA used to set the fixed target s_{tgt} . When enabled, we apply the fixed-target scale anchoring loss from Section 3.5 to the pre-logit residual stream with weight $\lambda = 0.1$ for all TinyStories runs. The target s_{tgt} is set to the bias-corrected EMA of the batch-mean scale during warmup and is held fixed after warmup.

D. GPT-2 fine-tuning details

This appendix summarizes the fine-tuning setup used in Section 5.3.

Data and tokenization. We fine-tune on the HuggingFace openwebtext dataset. We tokenize with the corresponding GPT-2 tokenizer, append an end-of-text token after each document, concatenate the token stream, and split into contiguous blocks of length 1024.

Optimization and schedule. We reuse the fine-tuning hyperparameters of Baroni et al. (2025). Training uses bf16, global gradient norm clipping with threshold 1.0, and a cosine learning-rate schedule with warmup. We use gradient accumulation to match a fixed global token batch size per optimizer step.

Taper schedule, EMA rates, and scale loss. Gates stay at $g = 1$ until taper start. At the taper start, each module freezes its alignment scalar c using EMAs of the quantities used for calibration (see Appendix B), copies $\gamma \rightarrow \tilde{\gamma}$, and then cosine-decays g to 0 over the taper window.

We use the same EMA update rate $\mu = 0.1$ (new-sample weight) while $g = 1$ (prior to taper start) for both (i) the calibration EMAs and (ii) the EMA used to set the fixed target s_{tgt} . The fixed-target scale loss weight is $\lambda = 0.1$ for GPT-2 Small/Medium/Large and $\lambda = 0.01$ for GPT-2 XL.

Evaluation. We reuse code published by Baroni et al. (2025) for evaluation and report cross-entropy on OpenWebText held-out blocks and on pre-tokenized subsets of The Pile and The Pile-filtered.